Integrated CFD and Digital Modeling Approach for Energy-Efficient Operation of Deep-Well Water Supply Systems

Mukhammadrasul Musajonov[1], Umar Chorshanbiev[1], Daniyar Tokanov[2], Durdona Obutjonova[1], Ahmadjon Ibadullaev[1], Oybek Muminov[3] and Vakhidjon Kholmirzaev[4]

[1]Tashkent State Transport University, Temiryolchilar Str. 1, 100167 Tashkent, Uzbekistan

[2]Abylkas Saginov Karaganda Technical University, Nursultan Nazarbayev Ave. 56, 100027 Karaganda, Kazakhstan

[3]Fergana State Technical University, Fergana Str. 86, 150100 Fergana, Uzbekistan

[4]Academy of Public Policy and Administration under the President of the Republic of Uzbekistan, Islom Karimov Str. 43, 100000 Tashkent, Uzbekistan

muhammadrasulmusajonov@gmail.com, umarttymikq25@gmail.com, durdonaobutjonova02@gmail.com, ibadullaev1957@bk.ru, d.tokanov@ktu.edu.kz, muminov.oybek@ferpi.uz, vohidholmirzaev@yandex.com

Keywords: Deep-Well Water Supply, CFD Modeling, ANSYS Fluent, Energy Efficiency, Digital Modeling, Hydraulic Optimization.

Abstract: Deep-well water supply systems are characterized by significant hydraulic losses and high energy consumption, especially at depths exceeding 150-200 m. Traditional design and operational approaches often rely on simplified hydraulic calculations, which limit the potential for energy optimization. This paper presents an integrated approach combining Computational Fluid Dynamics (CFD) modeling and digital monitoring concepts to improve the energy efficiency of deep-well water supply systems. A three-dimensional CFD model of the well-pump-pipeline system was developed using ANSYS Fluent to analyze flow behavior, pressure distribution, and hydraulic losses under different operating conditions. The simulation results were used to evaluate pump power demand and identify optimal flow regimes with reduced energy consumption. In addition, a digital modeling framework for real-time monitoring and operational optimization based on sensor data is proposed. The results demonstrate that CFD-based optimization enables a significant reduction in pressure losses and pump energy consumption compared to conventional calculation methods. The proposed integrated methodology provides a practical decision-support tool for the design and operation of energy-efficient water supply systems and contributes to the digital transformation of hydraulic infrastructure.

1 INTRODUCTION

Deep-well water supply systems are essential for providing reliable drinking and industrial water, particularly in regions with limited surface resources. Such systems are also closely related to engineering communications of buildings and municipal infrastructure [1]. Water extraction depths often exceed 150-200 m, leading to significant hydraulic losses and high energy consumption, especially in deep-well pumping systems [2], [3]. Conventional design methods based on one-dimensional calculations and empirical formulas [4] cannot adequately capture complex flow behavior, turbulence, and localized pressure losses, which restricts energy optimization. Advances in Computational Fluid Dynamics (CFD) enable detailed three-dimensional analysis of flow, pressure distribution, and energy dissipation in deep wells and pipelines [5]. CFD tools such as ANSYS Fluent provide more accurate assessment of the interaction between well geometry, pump operation, and pipeline characteristics than traditional approaches (Fig. 1) [6]. At the same time, digital transformation of infrastructure supports data-driven monitoring and optimization, where digital models integrated with real-time sensor data (digital twins) enable continuous system assessment and adaptive operational control [7], [8]. Despite extensive research on CFD and energy efficiency in water systems, limited attention has been given to integrated approaches combining CFD and digital modeling for deep wells. This study addresses this gap by developing a three-dimensional CFD model of a representative deep-well system and proposing a digital monitoring and optimization framework to improve energy-efficient operation. In this study, the term digital modeling is used in a practical engineering sense, referring to a CFD-informed digital monitoring model rather than a full-scale high-fidelity digital twin.

2 RELATED WORKS AND PROBLEM STATEMENT

Energy efficiency is a key factor for sustainable water supply systems [2]. Previous studies highlight energy reduction through improved hydraulic design, optimized pump selection, pump scheduling, and operational control [9], [10]. In deep-well systems, frictional, turbulent, and local losses strongly affect energy demand, while conventional one-dimensional models such as the Darcy-Weisbach equation [4] cannot adequately represent complex three-dimensional flow and localized energy dissipation near pumps and fittings. CFD has therefore been widely applied to pipelines, pumps, and networks to improve prediction of flow and pressure fields [5], [11]. However, most studies consider individual components rather than the integrated behavior of deep-well systems [12]. At the same time, digitalization of water infrastructure enables real-time monitoring and optimized decision-making [7], [8]. Since CFD and digital monitoring are often applied separately, their potential for continuous operational optimization remains limited. This study addresses this gap by proposing an integrated CFD-digital modeling framework to improve energy efficiency and support sustainable operation of deep-well water supply systems.

3 METHODOLOGY

This study adopts an integrated methodology combining Computational Fluid Dynamics (CFD), energy efficiency assessment, and digital modeling concepts to analyze and optimize the operation of deep-well water supply systems. The proposed approach enables detailed investigation of hydraulic behavior, accurate estimation of energy losses, and the development of digital decision-support tools for efficient system operation.

3.1 Physical and Hydraulic Model

The physical model is based on real operating conditions at the Kattakurgan District Branch of Samarkand Water Supply JSC and represents a typical deep-well water supply system. The research object includes a vertical artesian well, a submersible pump, and a rising pipeline supplying water to clean-water reservoirs and the centralized distribution network. In 2025, the district population was approximately 300,000, with about 65-70% connected to centralized water supply, making system reliability and energy efficiency critically important (Fig. 1). The branch operates around 600 km of drinking water pipelines and several pumping stations for groundwater extraction and pressure maintenance.

Figure 1: Layout of the deep-well water supply system at Kattakurgan District Branch.

The system includes vertical artesian wells with depths ranging from 50 m to 250 m, submersible pumps with capacities of 50-150 m^3/h, and rising pipelines made of polymer material with internal diameters of 300-500 mm. Water towers and reservoirs with a total storage capacity of 4,200 m^3 regulate pressure and store water reserves for approximately 65-70% of the 300,000 population connected to the network (research object).

The artesian wells have depths of 50-250 m; a representative well of about 200 m depth was selected for numerical analysis. The rising pipeline is assumed to be made of polymer material due to its corrosion resistance and favorable hydraulic performance. Water is modeled as an incompressible Newtonian fluid with constant properties. Flow in the system is governed by gravity, pump-generated pressure, and frictional and local hydraulic losses, which determine the required pumping head and energy consumption. This model provides the basis for subsequent CFD simulations aimed at assessing hydraulic losses and improving energy efficiency (Fig. 2).

Table 1: CFD modeling and digital monitoring framework for deep-well water supply system.

Parameter / Component	Description / Value	Purpose / Role
Geometry	Vertical artesian well (depth 200 m), submersible pump, rising pipeline	Physical representation of the system for CFD simulation
Mesh Type	Unstructured mesh with local refinement near walls	Accurate capture of flow near pump and bends
Mesh Size	Element size: 0.05-0.2 m (refined near pump and pipe bends)	Ensures mesh independence and resolution of flow features
y^+ Target	30-300 (wall function approach)	Appropriate near-wall turbulence modeling
Turbulence Model	Realizable k-ε model	Models internal turbulent flow efficiently
Fluid Properties	Water, incompressible, ρ = 1000 kg/m³, μ = 0.001 Pa·s	Physical properties for CFD calculation
Inlet BC	Mass flow rate (operational regimes: 0.05-0.15 m³/s)	Drives CFD simulation
Outlet BC	Pressure outlet, atmospheric pressure	Defines system boundary
Wall BC	No-slip, hydraulically smooth	Accurate representation of pipe walls
Convergence Criteria	Residuals < 1×10^{-5} for continuity, momentum, k, ε	Ensures numerical solution accuracy
Simulation Software	ANSYS Fluent 2023 R1	CFD solver used
Sensors	Pressure transducers, flow meters, water level sensors, energy meters	Real-time monitoring of operational parameters
Sampling Rate	1-5 s for flow/pressure; 10 s for energy meters	High-resolution data acquisition
Data Acquisition	PLC / SCADA system or IoT gateway	Collects and forwards sensor data to digital model
Data Pipeline	Cloud/local database (SQL/NoSQL), API endpoints	Stores, processes, and integrates CFD-derived optimal ranges
Digital Model	CFD-based operational envelopes, historical data analytics	Defines optimal operating regimes and predicts system behavior
Dashboard & Alerts	Web-based or SCADA interface, color-coded indicators, email/SMS alerts	Visualizes system state, warns operators of deviations
Control Actions	Pump speed regulation, flow control valves, automated alarms	Adjusts system operation to maintain energy-efficient performance

Figure 2: Electricity consumption of the deep-well water supply system from 2021 to 2025.

3.2 CFD Modeling Using ANSYS Fluent

A three-dimensional numerical model of the deep-well water supply system was developed using ANSYS Fluent to analyze hydraulic performance, pressure losses, and energy efficiency under different operational scenarios. The model incorporates the artesian well, submersible pump, and rising pipeline, reflecting actual field conditions observed at the Kattakurgan District Water Supply Branch (Fig. 3). To ensure clarity, reproducibility, and proper documentation for digital monitoring integration, the key CFD modeling parameters are summarized in Table 1.

The governing equations for mass and momentum conservation are based on the incompressible Navier-Stokes equations.

$$\nabla\cdot\vec{v}=0,$$
$$\rho(\vec{v}\cdot\nabla)\vec{v}=-\nabla p+\mu\nabla^2\vec{v}+\rho\vec{g}. \quad (1)$$

where $\vec{v}$ is the velocity vector, p is pressure, ρ is fluid density, μ is dynamic viscosity, and $\vec{g}$ represents gravitational acceleration. Turbulence effects were modeled using the realizable k-ε turbulence model, providing a good balance between computational efficiency and accuracy for internal turbulent flows. The computational domain was discretized using an unstructured mesh, with local refinement near the pipe walls to accurately capture boundary layer effects.

Boundary conditions are defined as follows:

- Inlet. Specified mass flow rate corresponding to different operational regimes.
- Outlet. Pressure outlet at atmospheric pressure.
- Walls. No-slip condition with hydraulically smooth surface assumption.

Mesh independence was evaluated using three different grid densities: a coarse mesh with approximately 0.9 million cells, a medium mesh with 1.7 million cells, and a fine mesh with about 3.2 million cells. The comparison of numerical deviations between grid densities was interpreted using standard engineering statistical assessment principles [13]. The predicted total pressure loss and average flow velocity varied by less than 2% between the medium and fine meshes, which was adopted as the mesh-independence criterion. Therefore, the medium mesh was selected for all simulations as a compromise between numerical accuracy and computational cost. Convergence criteria were satisfied when residuals fell below 10^{-5} for all governing equations. The CFD results were verified using measured operational data, including electricity consumption records and system operating parameters from the studied water supply facility. The deviation between CFD-predicted and measured energy consumption did not exceed 6-9%, confirming the adequacy of the numerical model for quantitative engineering analysis. A quantitative validation of the CFD model was performed by comparing simulation results with field measurements of flow rate, total head, and pump power.

Table 2: Validation of CFD predictions against field measurements.

Parameter	Measured value	CFD value	Deviation (%)
Flow rate (m^3/s)	0.10	0.104	4.0
Total head (m)	205	192	6.3
Pump power (kW)	240	225	6.2

Table 2 presents a quantitative comparison between CFD predictions and field measurements. The deviation for all key parameters does not exceed 6-9%, which confirms that the numerical model is reliable for quantitative assessment of hydraulic losses and energy consumption. Although advanced turbulence models such as SST k-ω are widely used for internal flow simulations [14], the realizable k-ε model was selected in this study due to its robustness and lower computational cost for large-scale engineering applications. Preliminary test simulations showed that differences between realizable k-ε and SST k-ω predictions of total pressure loss were within 3%, while the computational cost of SST k-ω was significantly higher.

3.3 Energy Efficiency Assessment

The energy performance of the deep-well system is evaluated based on the CFD-derived pressure losses and pump operating conditions. The required pump hydraulic power P_h is calculated as:

$$P_h=\rho g Q H, \quad (2)$$

where Q is the volumetric flow rate and H is the total dynamic head obtained from CFD results. The actual electrical power consumption P_e is determined by accounting for pump efficiency η_p:

$$P_e=P_h/\eta_p. \quad (3)$$

In this study, the pump efficiency (η_p) was taken as 0.75 based on commonly accepted industry standards for deep-well centrifugal pumps operating under steady-state conditions. This value represents a typical efficiency level reported in technical literature and ensures realistic estimation of electrical power consumption. Energy efficiency improvements are assessed by comparing the CFD-optimized operating regime with conventional design-based calculations. The relative energy saving E_s is expressed as:

$$Es = (P_e,conv - P_e,CFD) / P_e,conv \times 100\%, \quad (4)$$

where $Pe, conv$ is the electrical power obtained from conventional hydraulic calculations, Pe, CFD is the electrical power predicted under CFD-optimized conditions, and Es is the relative energy saving (%).

3.4 Digital Monitoring and Optimization Framework

To support continuous energy-efficient operation, a digital monitoring and optimization concept is proposed. The framework integrates CFD-based insights with real-time operational data acquired from sensors measuring pressure, flow rate, water level, and energy consumption (Fig. 3). The digital model serves as a decision-support tool by:

- comparing real-time data with CFD-predicted optimal ranges;
- detecting deviations indicating hydraulic inefficiencies;
- recommending operational adjustments, such as pump speed regulation or flow control.

CFD simulations define optimal operational envelopes with maximum velocity of 2.8 m/s near the pump and pressure range of 0.05-0.15 MPa; these values were derived from the CFD simulations presented in Section 4.1. Real-time sensor data, including flow rate (0.05-0.15 m³/s), pressure, water level, and energy meters, are continuously compared with CFD-derived targets. Alerts are triggered if deviations exceed ±5% of the optimal range, enabling automatic pump speed regulation and preventive maintenance actions.

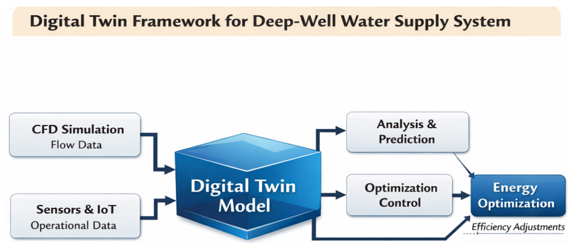

Figure 3: Integrated CFD-based digital monitoring framework for the deep-well water supply system.

This integration of numerical modeling and digital monitoring enables proactive system management and aligns with the principles of applied information technologies and smart infrastructure.

4 RESULTS AND DISCUSSION

4.1 Flow Field and Pressure Distribution

A CFD-based numerical modeling approach was developed to analyze the flow behavior and pressure distribution within the deep-well water supply system (Fig. 4). The obtained velocity contours represent the turbulent flow pattern in the deep-well vertical pipeline under normal operating conditions. The obtained pressure distribution (Fig. 4) demonstrates a nonlinear pressure variation due to gravitational and frictional effects.

Localized flow disturbances are identified in the vicinity of the pump outlet and transition zones, where changes in flow direction and cross-sectional geometry intensify turbulence levels.

Compared to conventional one-dimensional calculations, the CFD results demonstrate more accurate identification of zones with elevated pressure losses, particularly near the pump discharge region. These findings confirm that simplified hydraulic models tend to underestimate localized losses in deep-well systems.

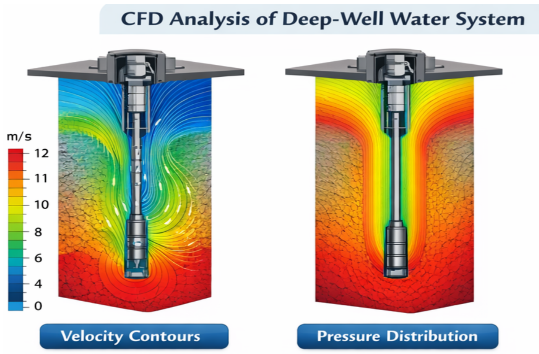

Figure 4: CFD-predicted velocity and pressure distributions in the deep-well pipeline.

4.2 Hydraulic Losses and Energy Consumption

Based on CFD-derived pressure data, the total dynamic head was calculated for different operating flow rates. The results show that hydraulic losses increase nonlinearly with increasing flow rate due to intensified turbulence and friction, a behavior not fully captured by conventional analytical methods.

A clear correlation exists between water supply volumes and electricity consumption. Analysis of operational data for 2021-2025 indicates that higher water production corresponds to increased electricity use, confirming that pumping units dominate energy consumption in the system (Fig. 5). The specific electricity consumption per 1 m³ of water was lower in 2022 and 2025, indicating improved energy efficiency, while higher values in 2021 and 2024 are likely related to less favorable pump operating regimes. Seasonal variations were also observed, with peak electricity consumption during summer months coinciding with increased water demand.

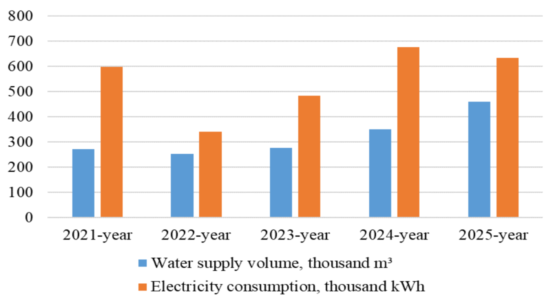

Figure 5: Water supply volume and electricity consumption from 2021 to 2025.

Comparison between CFD-based and conventional hydraulic calculations shows that the CFD approach predicts lower optimal operating heads for certain flow regimes. Consequently, total pressure losses were reduced by approximately 8-15%, leading to a corresponding decrease in pump energy consumption of about 10-18%. These results demonstrate the strong potential of CFD-based optimization for improving the energy efficiency of deep-well water supply systems. The average specific energy consumption of the system was approximately 0.76 kWh/m³.

4.3 Discussion of Energy Efficiency Improvements

Figure 6 illustrates the thermographic analysis of the electrical distribution panel, while Figure 7 presents temperature distribution on motors and cable connections. The observed energy savings are primarily due to the more accurate representation of flow behavior and hydraulic loss mechanisms provided by the CFD model. By identifying high-loss zones and optimal flow velocities, the analysis enables improved pump operating point selection and avoidance of overly conservative design margins. Even moderate reductions in pressure losses result in significant energy savings because of the high pumping head characteristic of deep-well systems. To complement the hydraulic assessment, thermographic inspection of the electrical power supply components was performed.

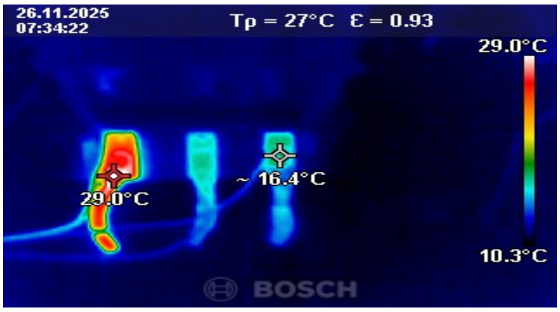

Figure 6: Thermographic analysis of the electrical distribution panel supplying pumps at Kattakurgan District Branch.

Temperature measurements show non-uniform heating, with maximum 29.0 °C at certain contact points, minimum 16 °C at less loaded sections, resulting in $\Delta T \approx 12\text{-}13$ °C. The uneven distribution indicates potential increases in contact resistance and localized overloading, which could reduce overall energy efficiency if not corrected.

The thermographic results revealed localized heating at certain contact and cable connection points, while most elements operated within normal temperature ranges. Although the detected temperature differences do not indicate a critical condition, they suggest increased contact resistance and potential electrical inefficiencies. Assessment of the induction motors showed generally uniform temperature distribution, confirming stable operation; however, minor overheating (up to 30.1 °C) was detected at specific cable sections, likely due to mechanical loosening.

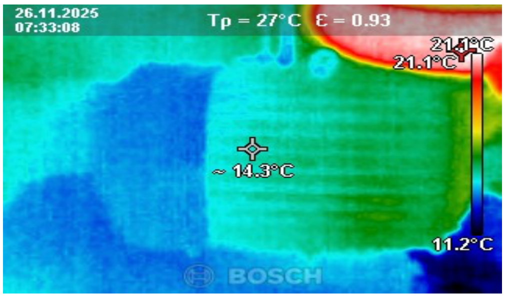

Figure 7: Thermographic assessment of induction motors and cable connections.

Maximum temperatures of 30.1 °C were observed at specific cable sections, while motor housings maintained uniform temperature of 27 °C. Localized heating corresponds to mechanical loosening and insufficient fastening, highlighting areas for preventive maintenance to avoid energy losses and improve operational reliability.

Overall, the combined CFD and thermographic analysis indicates that energy efficiency improvements depend not only on hydraulic optimization but also on the technical condition of electrical components. Electrical losses caused by contact resistance may partially offset hydraulic efficiency gains if preventive maintenance is not implemented. The CFD results provide the basis for the proposed digital monitoring and optimization framework. Pressure and velocity fields obtained from simulations define operational envelopes for efficient system performance. When combined with real-time sensor data, these envelopes allow continuous comparison between actual and optimal operating conditions. Integration of thermographic monitoring further improves system reliability. Periodic thermal diagnostics of electrical panels, motors, and cable connections enable early detection of electrical inefficiencies and prevention of additional energy losses. Deviations from CFD-predicted hydraulic behavior or detected thermal anomalies can trigger corrective actions, such as pump speed adjustment or preventive maintenance. This integrated approach shifts CFD from a purely design-stage tool to a dynamic element of a digital decision-support system. As a result, the combined use of CFD modeling, thermographic diagnostics, and digital monitoring enhances operational reliability and energy efficiency, supporting the practical application of digital technologies in water infrastructure management.

5 CONCLUSIONS

This study presented an integrated approach combining CFD, energy efficiency assessment, and digital modeling for the analysis and optimization of deep-well water supply systems. The methodology overcomes the limitations of conventional one-dimensional hydraulic calculations by providing a three-dimensional representation of flow behavior, pressure distribution, and localized hydraulic losses. CFD simulations using ANSYS Fluent enabled identification of high-loss zones and non-uniform pressure gradients along the well and rising pipeline, showing that traditional methods tend to underestimate localized losses. Energy performance analysis indicated that optimized operating regimes can reduce total pressure losses by approximately 8-15% and pump energy consumption by 10-18%, confirming the practical effectiveness of CFD-based optimization. In addition, a digital monitoring and optimization framework was proposed to support continuous, data-driven operation through integration of CFD results with real-time sensor data. Overall, the integrated CFD-digital modeling approach contributes to energy-efficient and sustainable water infrastructure management. Future research will focus on applying artificial intelligence and machine learning techniques for predictive maintenance, adaptive pump control, and full digital twin implementation, since AI-based tools are increasingly important for technological development and operational optimization [15]. The novelty of this study lies in the practical integration of CFD-derived hydraulic insights with a digital monitoring framework for operational optimization of deep-well systems.

REFERENCES

[1] M. A. U. Musajonov and D. Z. Umarova, “Engineering communications of buildings,” Issues of Science and Education, no. 8 (20), pp. 30-31, 2018.

[2] M. J. Ramos, J. A. Delgado, and A. Covas, “Energy efficiency in water supply systems: A review,” Renewable and Sustainable Energy Reviews, vol. 15, no. 8, pp. 3657-3668, 2011.

[3] M. A. El-Ghandour, “Energy consumption analysis of deep well pumping systems,” Energy and Buildings, vol. 43, no. 2-3, pp. 600-605, 2011.

[4] L. W. Mays, Ed., Water Distribution Systems Handbook. New York, NY, USA: McGraw-Hill, 2000.

[5] H. K. Versteeg and W. Malalasekera, An Introduction to Computational Fluid Dynamics: The Finite Volume Method, 2nd ed. Harlow, UK: Pearson Education, 2007.

[6] ANSYS, Inc., ANSYS Fluent Theory Guide, Release 2023 R1. Canonsburg, PA, USA, 2023.

[7] S. Menke, P. Abrahamsson, and J. Nylander, “Digital twins for water infrastructure: A review,” Water, vol. 13, no. 19, art. 2709, 2021.

[8] J. Wang, Y. Chen, and L. Zhang, “Integration of CFD modeling and real-time monitoring for smart water systems,” Sustainable Cities and Society, vol. 54, art. 101936, 2020.

[9] A. Covas and J. Ramos, “Case studies of energy optimization in water supply systems,” Journal of Water Resources Planning and Management, vol. 136, no. 2, pp. 205-213, 2010.

[10] A. J. Simpson and G. C. Dandy, “Energy efficient pump scheduling in water distribution systems,” Journal of Water Resources Planning and Management, vol. 135, no. 6, pp. 423-432, 2009.

[11] J. Wu, Z. Wang, and H. Li, “CFD analysis of pressure loss and flow characteristics in vertical pipelines,” Applied Thermal Engineering, vol. 102, pp. 800-809, 2016.

[12] S. Pezzinga and G. Brunone, “CFD modeling of transient flow in pressurized pipelines,” Journal of Hydraulic Engineering, vol. 137, no. 12, pp. 1625-1636, 2011.

[13] D. C. Montgomery and G. C. Runger, Applied Statistics and Probability for Engineers, 6th ed. Hoboken, NJ, USA: Wiley, 2014.

[14] E. Madaliev, M. Madaliev, S. Raxmankulov, and S. Raxmonkulova, “Turbulent mixing of two plane flows based on the SST turbulence model,” E3S Web of Conferences, vol. 452, art. 02012, 2023.

[15] M. A. Menshikova, G. P. Butko, A. V. Romantsov, and L. A. Ramenskaya, “Artificial intelligence and its importance for the development of the technological potential of an enterprise,” Bulletin of the Altai Academy of Economics and Law, no. 11-3, pp. 389-395, 2024.